Journal of Materials Chemistry

www.rsc.org/materials

Volume 22 | Number 21 | 7 June 2012 | Pages 10365–10940

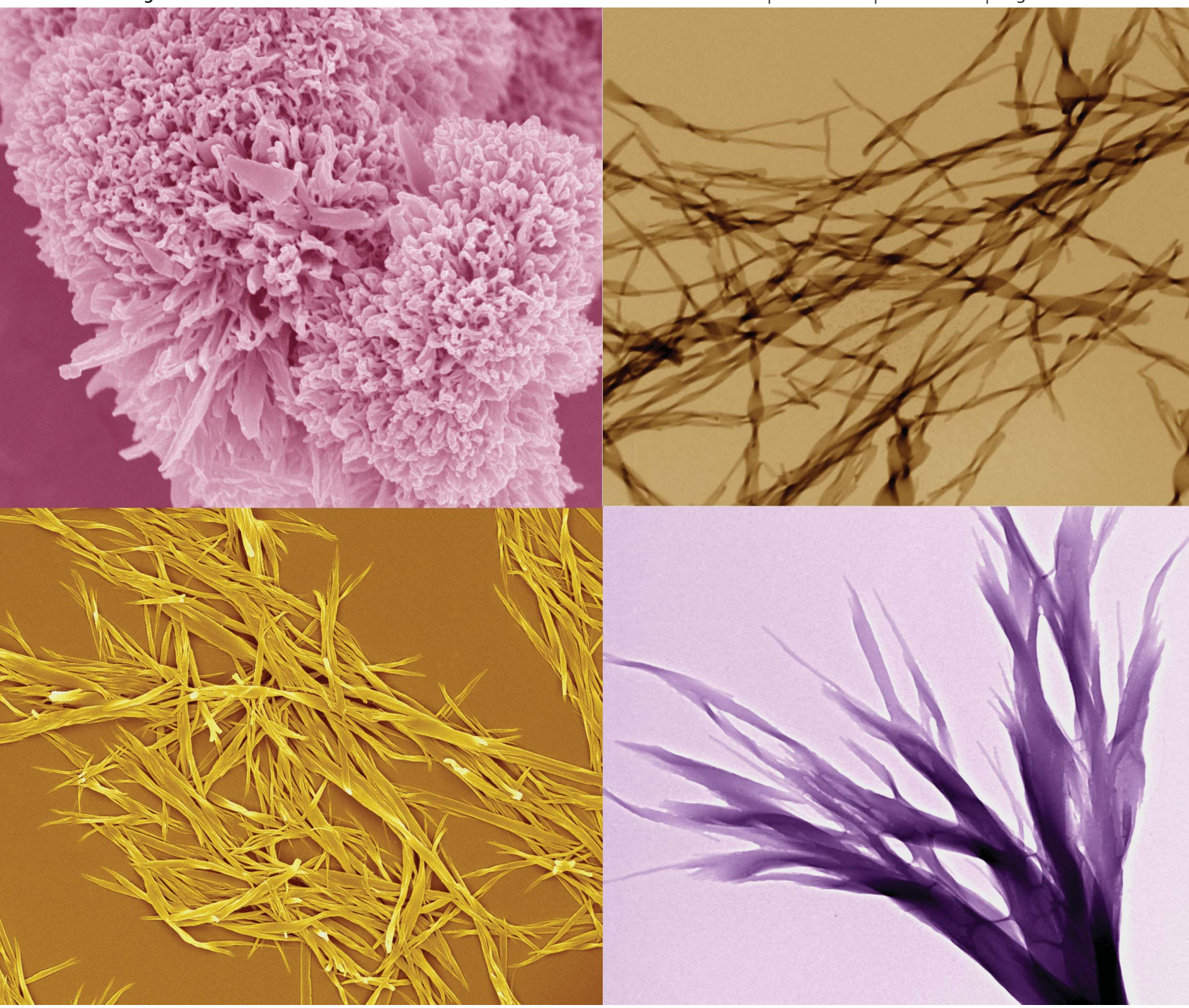

ISSN 0959-9428

RSC Publishing

PAPER

B. Z. Tang *et al.*

Synthesis and self-assembly of tetraphenylethene and biphenyl based AIE-active triazoles

0959-9428(2012)22:21;1-I

Journal of Materials Chemistry

Dynamic Article Links

Cite this: J. Mater. Chem., 2012, 22, 10472

www.rsc.org/materials

PAPER

Synthesis and self-assembly of tetraphenylethene and biphenyl based AIE-active triazoles†

Wang Zhang Yuan,[ab] Faisal Mahtab,[a] Yongyang Gong,[b] Zhen-Qiang Yu,[c] Ping Lu,[ad] Youhong Tang,[a] Jacky W. Y. Lam,[a] Caizhen Zhu[c] and Ben Zhong Tang*[a]

Received 1st February 2012, Accepted 13th March 2012
DOI: 10.1039/c2jm30620d

Self-assembly of fluorescent functional materials has attracted increasing interest in the fabrication of optoelectronic and biological nanodevices. Tetraphenylethene (TPE) is a typical dye molecule with aggregation-induced-emission (AIE) characteristics. Melding TPE carrying triple-bond functionality with diazide-containing biphenyl through "click" chemistry generates AIE-active luminogens [1,1′-biphenyl]-4,4′-diyl bis(6-(4-(4-(1,2,2-triphenylvinyl)phenyl)-1*H*-1,2,3-triazol-1-yl) hexanoate) [**1**(5)] and [1,1′-biphenyl]-4,4′-diyl bis(11-(4-(4-(1,2,2-triphenylvinyl)phenyl)-1*H*-1,2,3-triazol-1-yl) undecanoate) [**1**(10)] with solid state efficiencies up to unity. Slow addition of dilute THF solutions of **1**(*m*) (*m* = 5, 10) into nonsolvents such as *n*-hexane and water yields self-assembled white wooly solids. TEM and SEM observations reveal the (helical) nanofibrous structure of the aggregates. Upon cooling from their concentrated hot solutions, **1**(*m*) readily precipitate. Meanwhile, they can also form gels at high concentrations. Both precipitates and gels of **1**(*m*) exhibit structures similar to those of the aggregates formed in nonsolvents. These results indicate that **1**(*m*) can facilely self-assemble into high emission efficiency (helical) nanofibers, thus paving the way for their optoelectronic and biological applications.

Introduction

Intensive research has focused on the development of functional soft materials through molecular self-assembly in the past decades.[1–7] Landmark examples of hierarchical assemblies include micelles,[8] vesicles and liposomes,[9] microcapsules,[10] dendrimers,[11] gels,[12] and liquid crystalline materials.[3c,5a,13] Along these lines, self-assembly of π-conjugated molecules into linear structures has attracted much attention because of their potential applications in photonics and optoelectronics,[3a,6b,14–19] such as field-effect transistors (FETs),[15b,16,17] organic light emitting diodes (OLEDs),[18] organic light emitting transistors (OLETs),[17] and solar cells.[19] One-dimensional molecular assemblies can be constructed through weak intermolecular interactions such as hydrogen bonding, π–π stacking, electrostatic interactions, van der Waals forces, and solvophobic interactions.[4c,6b,14–20] As a matter of fact, optoelectronic device performances are highly dependent on the intermolecular order and/or emission efficiency in the active layers.[15b,20,21] Therefore, development of luminogens capable of self-assembling with high solid state efficiencies is of crucial importance.

Fabrication of one-dimensional (1D) nanostructures is attracting considerable interest in the field of nanotechnology due to their unique morphology, optical and electrical properties, and intriguing applications in electronics, sensors, and photonic materials.[3a,15b,20–22] Amongst varying nanostructures of fibers, wires, rods, belts, tubes, spirals, and rings, nanofibers are presently attracting increasing attention due to their specific properties and various applications in medical products, capacitors, transistors, drug delivery, battery separators, energy storage, fuel cells, and information technology.[4c,23]

Numerous methods have been demonstrated for generating nanofibers,[24] among which self-assembly affords an effective way towards novel materials with molecularly defined properties which are inaccessible through step-by-step synthesis.[6b,4c,15b,15d,20] Self-assembled nanofibers show peculiar, fascinating, and tunable properties, as well as unique applications in optoelectronically and biologically active materials.[7a,7b,16b,20,25–28] Therefore, it is of both fundamental and technological importance to craft diverse new functional nanofibers *via* self-assembly processes.

Compared with a variety of counterparts, fluorescent nanofibers are of particular interest.[25–29] Due to their luminescent features, fascinating photophysical behavior, and high aspect ratio, they are widely used in waveguidings,[25a] frequency

[a]*Department of Chemistry and State Key Laboratory of Molecular Neuroscience, The Hong Kong University of Science & Technology, Clear Water Bay, Kowloon, Hong Kong, China. E-mail: tangbenz@ust.hk*
[b]*School of Chemistry and Chemical Engineering, Shanghai Jiao Tong University, Shanghai 200240, China*
[c]*School of Chemistry and Chemical Engineering, Shenzhen University, Shenzhen 518060, China*
[d]*State Key Laboratory of Supramolecular Structure and Materials, Jilin University, Changchun 130023, China*

† Electronic supplementary information (ESI) available: Synthetic procedures, PL spectra of **1**(10) in THF and THF–water mixture, DSC data, and other materials. See DOI: 10.1039/c2jm30620d

doublers,[25b] nanolasers,[25c] chemo-[7a,30] and biosensors,[28] light-harvesting nanomaterials,[31] and OLEDs.[32] Despite their wide and important applications, fabrication of highly fluorescent nanofibers with optimal optoelectronic properties has proven to be a daunting job. It is because the notorious concentration quenching (CQ) and aggregation-caused quenching (ACQ) effects, which are usually encountered when luminophores are condensed and aggregated,[33] owing to the formation of detrimental excimers or exciplexes.

Our group is interested in the fabrication of high efficiency solid emitters, particularly those with aggregation-induced emission (AIE) characteristics,[34] which is contrary to the ACQ effect. Because highly active intramolecular rotations of the luminogens effectively consume the exciton energy, AIE-active molecules are practically nonfluorescent when molecularly dissolved in solvents; however, they become strong emitters upon aggregation owing to the restricted intramolecular rotations (RIRs).[34] Utilizing AIE-active molecules to fabricate self-assembled fluorescent nanofibers will be interesting in terms of their applications in biological, chemical, and optoelectronic devices.

Herein, we report the synthesis and self-assembly properties of tetraphenylethene (TPE) and biphenyl based triazoles **1**(5) and **1**(10) (Chart 1). Both luminogens are AIE-active, with solid state emission efficiencies up to unity. They are also capable of self-assembling into crystalline nanofibers by addition of their solutions into nonsolvents or upon cooling from their condensed hot solutions to room temperature or 4 °C. Moreover, these nanofibers are twisted and even helical though they are devoid of any chiral centers. A comparison experiment indicates that flexible spacers are of crucial importance in the formation of such helical structures.

Experimental

Materials

THF and toluene were distilled under normal pressure from sodium benzophenone ketyl under argon immediately prior to use. Other solvents, such as chloroform, hexane, and dimethylsulfoxide (DMSO), were of high purities and used as received. 4-(2-(Trimethylsilyl)ethynyl)benzophenone (**3**) was synthesized according to our previous procedures.[35] *p*-Toluenesulfonic acid monohydrate (TsOH), *N*,*N*′-dicyclohexylcarbodiimide (DCC), 4-dimethylaminopyridine (DMAP), 6-bromohexanoic acid [**7**(5)], 11-bromoundecanoic acid [**7**(10)], 4,4′-biphenol (**8**), sodium azide, and 1 M tetrabutylammonium fluoride (TBAF) in THF with 5% water were purchased from Aldrich and used without further purification. $Cu(PPh_3)_3Br$ catalyst was prepared according to the literature method.[36]

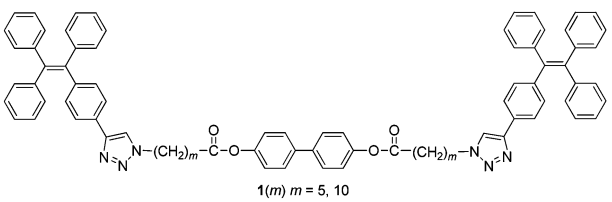

Chart 1 Chemical structure of **1**(*m*) (*m* = 5, 10).

Instrumentations

^1H and ^{13}C NMR spectra were measured on a Bruker ARX 400 spectrometer using $CDCl_3$ or DMSO-d_6 as solvent and tetramethylsilane (TMS) as internal standard. Matrix-assisted laser desorption/ionization time-of-flight (MALDI-TOF) high-resolution mass spectra (HRMS) were recorded on a GCT premier CAB048 mass spectrometer. Absorption spectra were taken on a Milton Roy Spectronic 3000 Array spectrometer. Emission spectra were taken on a Perkin-Elmer LS 55 spectrofluorometer. Transmission electron microscopy (TEM) and scanning electron microscopy (SEM) images were observed using JOEL 2010 TEM and JOEL 6700F SEM instruments at accelerating voltages of 200 and 5 kV, respectively. Samples were prepared by drop casting of dilute aggregate dispersions onto copper 400-mesh carrier grids covered with carbon-coated Formvar films. The solvent was evaporated at room temperature in open air. Thermal transitions were investigated by a TA DSC Q1000 under nitrogen at a heating rate of 10 °C min^{-1}. One-dimensional wide-angle X-ray diffraction (1D-WAXD) powder experiments were performed on a Philips X'Pert Pro diffractometer with a 3 kW ceramic tube as the X-ray source (Cu K_α) and an X'celerator detector. The sample stage was set horizontally and the samples were protected by nitrogen gas during the measurements. The reflection peak positions were calibrated with silicon powder ($2\theta > 15°$) and silver behenate ($2\theta < 10°$). Background scattering was recorded and subtracted from the sample patterns.

Synthesis

Compounds **1**(*m*) (*m* = 5, 10) and **11** were prepared through multistep reactions as shown in Schemes 1 and S1 (ESI†). Detailed procedures for the syntheses of the reaction intermediates are described in the ESI†. The final products **1**(*m*) were

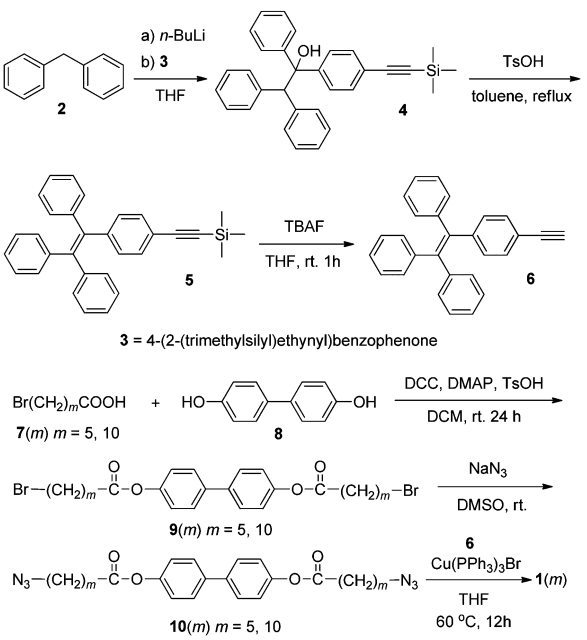

Scheme 1 Synthetic route to **1**(*m*) (*m* = 5, 10).

synthesized by "click chemistry" reaction, and the synthetic procedure of **1**(5) is given below as an example.

*Synthesis of [1,1′-biphenyl]-4,4′-diyl bis(6-(4-(4-(1,2,2-triphenylvinyl)phenyl)-1H-1,2,3-triazol-1-yl) hexanoate) [**1**(5)].* In a 15 mL Schlenk tube 46.5 mg (0.1 mmol) of **10**(5), 78.4 mg (0.2 mmol) of **6** and 2.8 mg of $Cu(PPh_3)_3Br$ were placed. 2 mL of THF was then injected. The reaction mixture was stirred at 60 °C and found to be gelated 12 h later. The crude product was purified by a silica gel column using a chloroform–acetone mixture (15 : 1 by volume). A white solid of **1**(5) was obtained in 90.1% yield. ^{1}H NMR (400 MHz, $CDCl_3$), δ (TMS, ppm): 7.71 (s, 2H, triazole protons), 7.57 (d, 4H), 7.52 (d, 4H), 7.13, 7.09, 7.07, 7.05, 7.04, 7.02, 4.42 (t, 4H, triaozle-CH_2), 2.59 (t, 4H, OOCCH_2), 2.01 (m, 4H, triaozle-CH_2CH_2), 1.82 (m, 4H, $OOCCH_2CH_2$), 1.48 (m, 4H, $OOCCH_2CH_2CH_2$). ^{13}C NMR (100 MHz, $CDCl_3$), δ (TMS, ppm): 171.83 (*C*=O), 150.08, 143.73, 143.64, 143.59, 143.53, 141.28, 140.42, 138.08, 131.85, 131.36, 131.31, 128.53, 128.13, 127.76, 127.68, 127.62, 126.52, 126.50, 126.45, 124.98, 121.83, 50.05 (triazole-*C*H_2), 33.97 (OOC*C*H_2), 30.01 (triazole-CH_2*C*H_2), 25.90 ($OOCH_2$CH_2), 24.15 ($OOCH_2CH_2$CH_2). HRMS (MALDI-TOF): calcd for $C_{80}H_{68}N_6O_4$: 1176.5302. Found: 1199.4940 $[M + Na]^+$.

Sample preparation for AIE measurement

Stock THF solutions of the luminogens with a concentration of 2×10^{-4} M were prepared. Aliquots of the stock solution were transferred to 10 mL volumetric flasks. After appropriate amounts of THF were added, water was added dropwise under vigorous stirring to furnish 2×10^{-5} M solutions with different water fractions (0–90 vol%). PL measurement of the resulting solutions or suspensions was then performed immediately.

Quantum yield determination

Quantum yields ($\Phi_{F,s}$) of **1**(*m*) (*m* = 5, 10) in THF were estimated using 9,10-diphenylanthracene (Φ_F = 90% in cyclohexane) as standard (excitation wavelength = 270 nm), while the $\Phi_{F,f}$ values of solid powders were determined using an integrating sphere.

Visual molecular dynamics simulation

To obtain theoretical understanding of the molecular interactions and to get insights into the self-assembly mechanism, molecular dynamic simulation of **1**(5) was conducted. The snapshots for all figures were taken with Visual Molecular Dynamics (VMD),[37] a famous visualization tool to view MD simulation results, and the structure was modeled by the self-defined script.

Results and discussion

Scheme 1 illustrates the synthetic routes to the resulting compounds **1**(*m*). Detailed procedures and characterization data are given in ESI†. Briefly, important intermediate **6** was prepared by lithiation of **2**, followed by coupling with 4-(2-(trimethylsilyl) ethynyl)benzophenone (**3**), dehydration,[38] and cleavage of trimethylsilyl group in basic medium. Meanwhile, esterification of 4,4′-biphenol (**8**) with ω-bromoalkanoic acid **7**(*m*) in the presence of DCC, DMAP, and TsOH yielded compounds **9**(*m*), which were then reacted with sodium azide, furnishing the desirable key intermediates **10**(*m*). The target triazoles **1**(*m*) were obtained through facile "click chemistry" reaction catalyzed with $Cu(PPh_3)_3Br$ in THF at 60 °C. All reactions proceeded smoothly and the desirable compounds were obtained in high yields. The compounds were characterized by standard spectroscopic methods, from which satisfactory analysis data corresponding to their molecular structures were obtained (ESI†).

1(10) shows an absorption profile almost identical to that of **1**(5) with an absorption maximum at 322 nm (Fig. 1), which is corresponded to the π–π* transition of the TPE-based triazoles. When illuminated with a UV lamp, neither of their solutions emits any observable light but strong blue light from their solid powders and thin films, suggesting that aggregation has turned on their emissions. To verify it, the emission spectra of **1**(*m*) in THF and THF–water aqueous mixtures were measured. Water is used since it is a nonsolvent of **1**(*m*): the luminogen molecules must aggregate in the aqueous mixtures with high water fractions (f_w). Take **1**(5) for example, weak PL signals are recorded even when the f_w is as high as 50% because the **1**(5) molecules are still molecularly dissolved in these mixtures (Fig. 2). The PL intensity starts to rise at f_w > 60% and, at much higher f_w (≥80%), slight increase in f_w gives abrupt promotion in emission intensity,

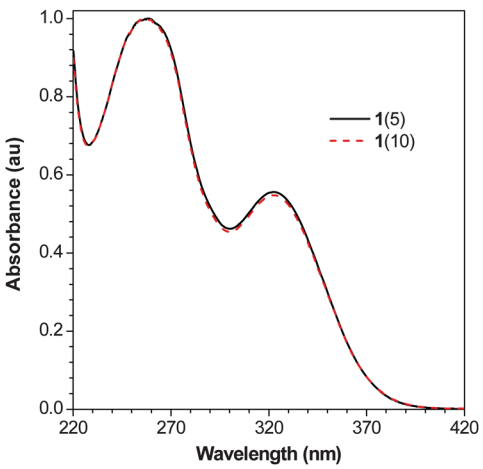

Fig. 1 Normalized absorption spectra of **1**(5) and **1**(10) in THF. Concentration = 20 μM.

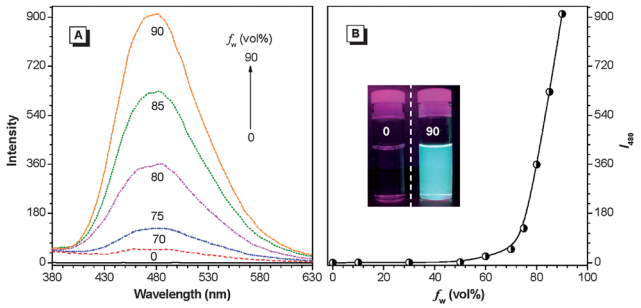

Fig. 2 (A) Emission spectra of **1**(5) in THF and THF–water mixtures. (B) Plot of emission peak intensity at 480 nm *vs.* f_w of the aqueous mixture. Concentration = 20 μM; excitation wavelength = 340 nm. Inset: photographs of **1**(5) in THF–water mixtures with f_w values of 0% and 90% taken under UV illumination.

suggesting that the luminogen molecules are seriously aggregated in such aqueous media. Fig. 2B shows the emission peak intensities at varying water fractions. Clearly, from the molecular solution in THF to the aggregate suspensions in 90% aqueous mixture, the emission intensity of **1**(5) at 480 nm is increased by ~5944 times. Similar behaviors are also observed for **1**(10), whose peak emission enhancement upon adding 90% water is as high as ~7819 times (Fig. S1, ESI†). Evidently, both luminogens of **1**(5) and **1**(10) are AIE active. Moreover, such high emission enhancement values are quite impressive among those reported for other AIE molecules.[39]

To further validate the AIE activity of **1**(*m*), their emission quantum efficiencies (Φ_F's) in THF solutions and solid states were determined. The $\Phi_{F,s}$ values of **1**(5) and **1**(10) in THF are as low as 0.54% and 0.52%, whereas those of their solid powders ($\Phi_{F,f}$) are both boosted to 100% by aggregate formation, resulting in AIE factors ($\alpha_{AIE} = \Phi_{F,f}/\Phi_{F,s}$) as high as 185.2 and 192.3, respectively. Similar to previous systems, the AIE behavior of **1**(*m*) should be ascribed to RIR mechanism of the chromophores.[34,39–41] Namely, the molecularly dissolved species of **1**(*m*) in solvents undergo active intramolecular rotations owing to their highly twisted configurations of TPE based triazoles. These rotations effectively dissipate the excitons energy, making the luminogens nonemissive in solutions. However, when they are aggregated as nanosuspensions, powders, or solid thin films, the intramolecular rotations are strikingly impeded; meanwhile, their propeller-like structure prevents the formation of detrimental excimers or exciplexes, thus endowing the aggregates with intense emissions.

We are interested in fabrication of high efficiency luminescent liquid crystals.[34g,34h] To check whether **1**(*m*) are liquid crystals, POM observation was conducted but only a negative result was obtained. However, accidentally, when THF solutions of **1**(*m*) were dropped into *n*-hexane, flocculent precipitates were instantaneously formed (Fig. 3A and B). Morphologies of the precipitates were characterized by TEM and SEM, and characteristic images are presented in Fig. 3C–F. TEM image of **1**(5) reveals the formation of ribbon-like nanofibers, with lengths of several micrometres and widths ranging from 30 to 100 nm (Fig. 3C). Similar morphologies with well developed fibrillar structures are also observed for **1**(10) (Fig. 3D). SEM images show the entangled 3-dimensional networks consisting of fibrous nanostructures for the flocculent precipitates. The formation of such elongated nanofibers suggests that self-assembly of **1**(*m*) is driven by the strong directional intermolecular interactions.

Generally, nanofibers are taken as an intermediate state between molecularly dissolved species and organogels upon increasing the concentration.[42] The strong tendency of **1**(*m*) to self-assemble into nanofibers inspired us to investigate their gelation capability. It is known that gelation behavior of a compound is strikingly dependent on its inherent properties, solvent, temperature, concentration, cooling rate, *etc.* Several solvents, such as cyclohexane, THF, DCM, and DMSO, were tested. Both compounds were insoluble in cyclohexane even at elevated temperatures. They were soluble in DCM and DMSO at low concentrations, but would precipitate upon cooling from their concentrated hot solutions. Differently, they showed high solubility in THF at ambient conditions, in which their gelation abilities were tested. The concentrated solutions of **1**(*m*) were

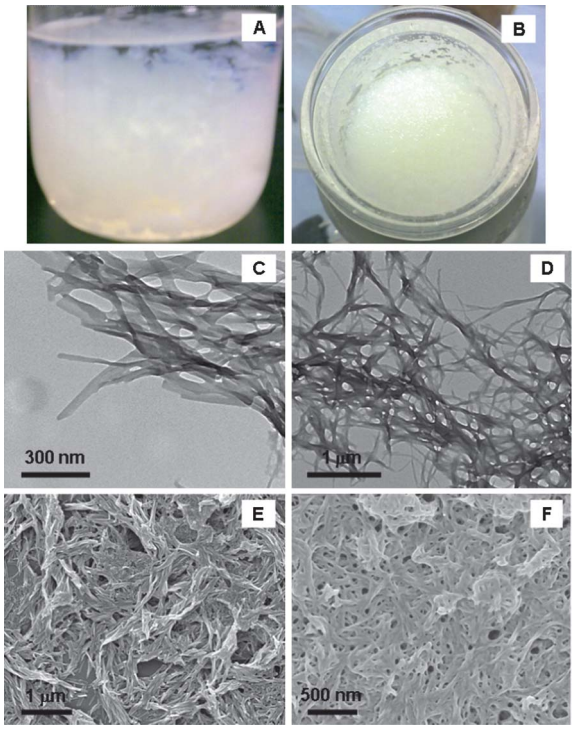

Fig. 3 (A and B) Photographs for flocculent precipitates of **1**(10) in *n*-hexane. (C and D) TEM and (E and F) SEM morphologies of the flocculent precipitates of (C and E) **1**(5) and (D and F) **1**(10) formed by dropping their THF solutions (1 mg mL^{-1}) into *n*-hexane.

obtained at elevated temperatures. However, no gel but a small amount of precipitates were formed for 20 mg mL^{-1} **1**(10) when cooled from 60 to 4 °C. Further increasing the concentration to 50 mg mL^{-1}, still no gelation occurred. However, typical gels were formed at a much higher concentration of 60 mg mL^{-1}. For **1**(5), whose hydrophobic chain is much shorter than **1**(10), only when the concentration was as high as 90 mg mL^{-1}, gels could be formed, indicating that a much longer spacer length is favored for the gelation process.

Fig. 4 shows the TEM and SEM images of the gel and precipitates formed in THF. As shown in Fig. 4A and D, fibrous helical nanostructures are formed for the gel of **1**(10). **1**(5) and **1**(10) precipitates exhibit similar fibrous structures (Fig. 4B, E, C and F), suggesting the strong tendency of **1**(*m*) to form ordered (helical) nanofibers, which might be resulted from the hydrophobic interactions between flexible spacers and effective interactions between intermolecular biphenyl and TPE units.

Self-assembly of TPE derivatives and other AIE-active luminogens into needle-like microcrystals,[40a] fibrils,[26] nanorods,[43] and nanorings[44] was previously reported; however, helical nanofibers were scarcely present. Herein, the nanofibrous structure of gels and precipitates of **1**(*m*) should be highly related to the internal alkyl chain substituted biphenyl units; however, the ordered nanostructures also strongly suggest the regular packing of TPE luminogens.

1(*m*) can form nanofibers upon precipitation and gelation. Such strong tendency to self-assemble into ordered 1D nanostructures implies the effective molecular association, which might be an inherent attribute of **1**(*m*). To verify it, THF solution

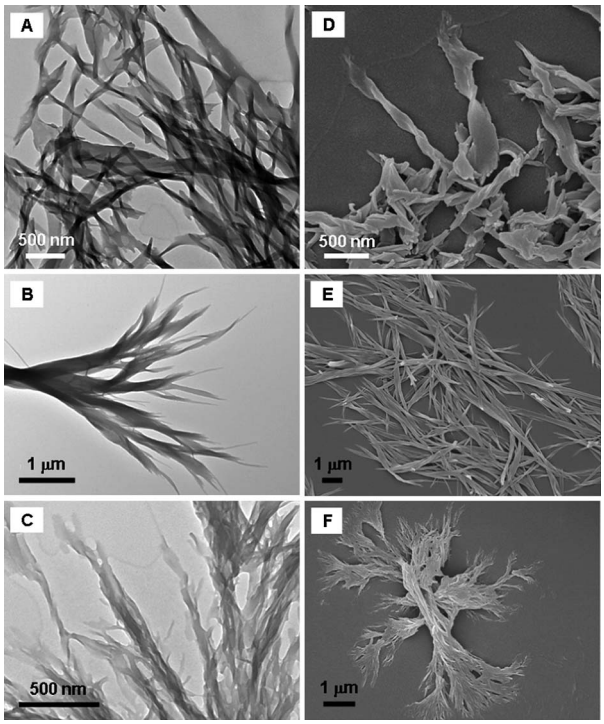

Fig. 4 (A–C) TEM and (D–F) SEM morphologies for (A and D) the gel of **1**(10) formed in THF and precipitates of (B and E) **1**(5) and (C and F) **1**(10) generated from their concentrated hot THF solutions upon cooling.

of **1**(10) was slowly dropped into water. Once the solution was diffused into water, white turbid mixture was formed, then these small white precipitates attached together to form wooly solids when further solution drops were added, finally giving a clear aqueous mixture with white flocculent precipitates in it. Such phenomenon is quite similar to that observed in *n*-hexane–THF system. The SEM images of the precipitates are given in Fig. 5. Apparently, sea chestnut-like spheres consisting of numbers of nanofibers were formed in water. It is reasonable to speculate that **1**(10) initially assembled into nanofibers due to its inherent insolubility in water, then emerged together to form spherical particles to minimize their surface energies. The result indicates that it is a general phenomenon that **1**(*m*) can self-assemble into nanofibers or even helical fibrous structures, thereby confirming the above conjecture.

It is also notable that helical structures may endow the aggregates with optical active properties; however, no obvious signal was recorded in circular dichroism (CD) measurement for the nanofibrous suspensions, indicating statistically equal ensemble of left and right handed conformations.

X-ray diffraction measurement was also conducted to evaluate the supramolecular nanoassemblies. Fig. 6 presents the X-ray powder diffractograms for varying precipitates of **1**(*m*) obtained in *n*-hexane, THF, and water. Evidently, all spectra display similar crystal profiles, suggesting the crystalline nature of the precipitates. However, while peaks at 2θ of ~1.76 and 1.73° for **1**(5) and **1**(10) suggest long-range-ordered arrangements of the aggregates, the absence of sharp and narrow peaks indicates that the molecular packing of **1**(*m*) is not as good as that in single crystals. According to Bragg's equation, *d*-spacings of the aggregates for **1**(5) and **1**(10) in *n*-hexane are estimated to be 51.07 and 51.67 Å, respectively, which are comparable to their extended molecular lengths (50.13 and 62.54 Å for **1**(5) and **1**(10), Chart S1, ESI†), suggesting the monolayer packing of the molecules. In the wide-angle region, broad peaks with corresponding *d*-spacings of ~4.5 Å are assignable to molecular stacking between adjacent TPE units. Meanwhile, signals of the precipitates obtained in *n*-hexane are relatively well reserved, thereby indicating a much better molecular packing in it.

Generally, self-assembly processes can be controlled both kinetically and thermodynamically. THF and water are typical solvent and nonsolvent for **1**(*m*), respectively. While **1**(*m*) can be molecularly dissolved in THF, they must aggregate in THF–water aqueous mixtures with high f_w due to the decreased solvating power. Therefore, in aqueous media with gradually changed THF and water fractions, **1**(*m*) should be present in varying forms. For example, during the AIE measurement experiment, in the 10/90 THF–water system, **1**(*m*) molecules must immediately aggregate when a large amount of water is added into the THF stock solution, forming kinetically stable nanosuspensions. Specifically, in the systems with inflexional solvating power for **1**(*m*), though the molecules started to aggregate, giving slight increase in PL intensity, there was still a considerable amount of molecules dispersed in the mixture. These molecules can steadily assemble into more stable and more ordered agglomerations. Indeed, during our experiment, the 10/90 THF–water system remained unchanged for days once

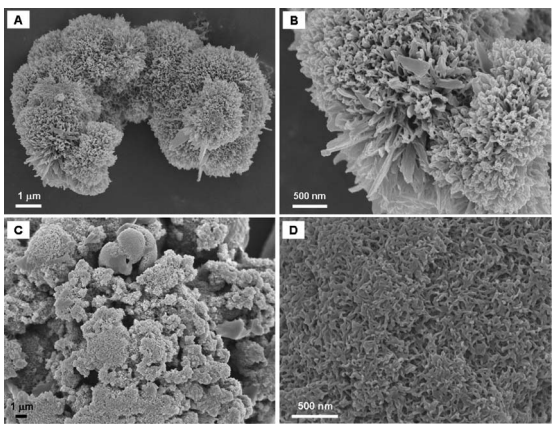

Fig. 5 SEM morphologies of the flocculent precipitates of **1**(10) formed by dropping its THF solution (1 mg mL^{-1}) into water.

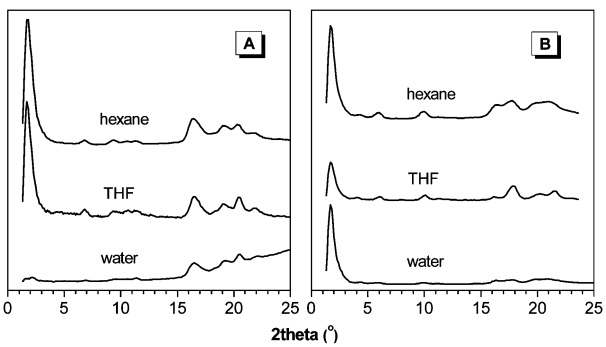

Fig. 6 WAXD powder diffractograms for varying precipitates of (A) **1**(5) and (B) **1**(10) generated in *n*-hexane, THF, and water.

the nanosuspensions were formed, whereas the 40/60 system changed from an initially transparent mixture to a white solid-containing heterogeneous admixture upon standing for 6 h. Meanwhile, the emission intensity of **1**(*m*) was also remarkably enhanced with the formation of white solids due to the AIE feature of the molecules.

TEM observation discloses the morphology of the aggregates in 10/90 and 40/60 THF–water aqueous media. As depicted in Fig. 7A and B, fine nanoparticles with diameters ranging from several tens to ~200 nm were formed in the 10/90 mixtures for both molecules. However, well reserved helical nanofibers with the length of several micrometres and the width of ~100 nm were formed for the 40/60 system of **1**(5) upon standing (Fig. 7C and D). These results clearly suggest that the helical nanofibers are thermodynamically stable aggregates for **1**(*m*) during the self-assembly process, whereas the nanoparticles in 10/90 THF–water mixture are only kinetically controlled agglomerations, whose further morphology developing is highly restricted due to the freezing of the molecules.

Emission spectra were also obtained for the nanoparticles and helical nanofibers. As shown in Fig. 7E and F, PL spectrum for the nanoparticles of **1**(5) exhibits an emission maximum at 480 nm, whereas that of the helical fibers peaks at 455 nm, giving a large blue shift of 25 nm. Further excitation of such aggregates with different wavelengths gives almost identical emission peaks (ESI†). Therefore, the emission peak difference of **1**(5) in 10/90 and 40/60 THF–water aqueous mixtures might be ascribed to the change in the packing mode of the dye molecules in aggregates. In 40/60 mixture, the dye molecules steadily assembled into ordered crystalline nanofibers. In 10/90 mixture, however, the dye molecules quickly agglomerated in a random way to form amorphous particles. The amorphous TPE molecules may adopt more planar conformations and hence exhibit redder emissions than those in the crystalline state.[45]

To evaluate the effect of flexible spacers on the formation of helical nanofibers, a congenerous compound of **1**(*m*), namely **11** (Fig. 8A), without alkyl chains was designed and successfully synthesized (Scheme S1, ESI†). The solubility of **11** is low in THF, chloroform, and DCM, and moderate in DMF due to its rigid skeleton and strong intermolecular interactions. For comparison, slow evaporation of the dilute THF solution of **11** and a precipitation experiment by dropping its THF–DMF (8/2, v/v) solution into *n*-hexane nonsolvent were conducted. The morphologies of the resulting precipitates were observed by TEM, and the results are shown in Fig. 8B–D. Apparently, different to what has been observed in the systems of **1**(*m*), crystalline particles (Fig. 8B) or nanosheets (Fig. 8C and D) rather than helical nanofibers were generated during the aggregation processes, thus proving the crucial role of flexible spacers in the formation of helical aggregations.

To get further insights into the self-assembly processes and mechanism, visual molecular dynamics simulation (VMDS) of **1**(5) was conducted. As shown in Fig. 9, adjacent **1**(5) molecules were packed together through effective intermolecular

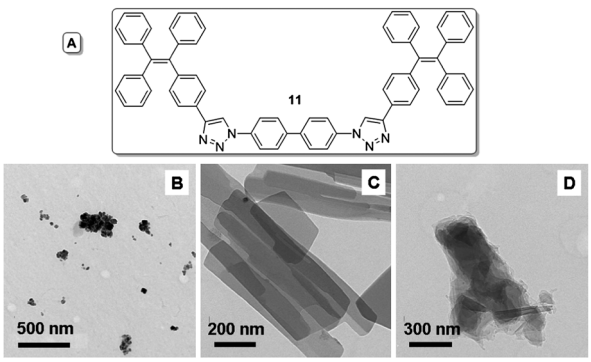

Fig. 8 (A) Chemical structure of compound **11** and TEM morphologies of the aggregates of **11** obtained by (C) slow evaporation of its dilute THF solution (0.1 mg mL^{-1}) and (C and D) dropping its THF–DMF (8/2, v/v) (1 mg mL^{-1}) solution into *n*-hexane.

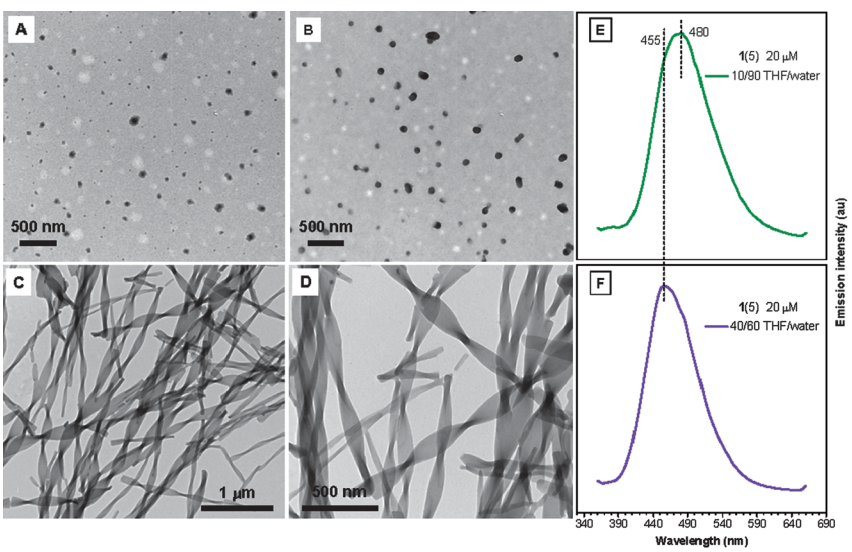

Fig. 7 TEM images for the aggregates of (A) **1**(5), (B) **1**(10) formed in 10/90 THF–water aqueous media and (C and D) the precipitates of **1**(5) in THF–water mixture (40/60) formed upon standing for 6 h. Normalized emission spectra for (E) the nanosuspensions and (F) helical nanofibers of **1**(5) in 10/90 and 40/60 THF–water aqueous media. Excitation wavelength = 340 nm.

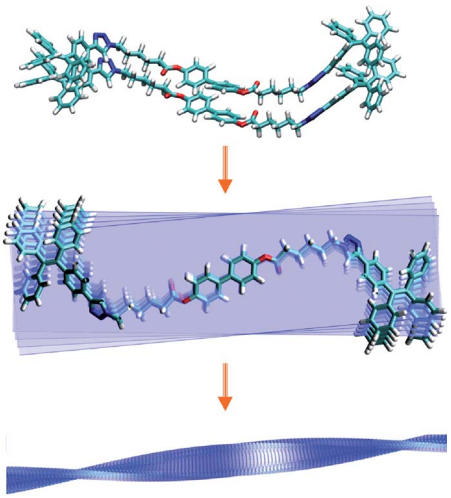

Fig. 9 A possible packing motif of **1**(5) and a mechanism for the formation of helical nanofibers.

interactions. Whilst biphenyl and TPE units are stacked face to face, they favor the formation of assemblies with tiny twist angles due to their nonplanar configurations and moreover the presence of flexible connection chains. Such twistingly packed molecules finally produce mesoscopic helical fibrous aggregates. The simulation result provides theoretical information on the self-assembly process of **1**(*m*), which is in good agreement with the experimental data. The disclosure of such mechanism of AIE-active **1**(*m*) will be instructive for us to design more functional molecules capable of self-assembling into high efficiency fluorescent helical nanofibers in future.

Conclusions

Biphenyl and TPE-containing luminogens **1**(*m*) are facilely synthesized and well characterized. Both compounds are practically nonluminescent in solutions, but become highly fluorescent when aggregated as nanosuspensions, solid powders, or thin films, exhibiting typical AIE characteristics, with the solid state emission efficiencies up to unity. Meanwhile, **1**(*m*) molecules can self-assemble into crystalline helical fibrillar nanostructures through gelation or simple precipitation processes, although they are devoid of any chiral centers. Such a strong self-assembly tendency of **1**(*m*) has proven to be an inherent nature of molecules owing to the effective intermolecular interactions. A comparison experiment suggests the crucial role of flexible spacers in the formation of helical nanoaggregates. High solid state efficiency and inherent self-assembling capacity of **1**(*m*) make them promising candidates for optoelectronic and biological nanodevices. Particularly, this work provides a new family of luminophors which can be facilely fabricated as high efficiency fluorescent (helical) nanofibers with AIE characteristics, thus overcoming the ACQ problem that normally occurs in preparing emissive nanofibers.

Acknowledgements

We thank the support from the Research Grants Council of Hong Kong (603509, HKUST2/CRF/10, and 604711), the NSFC/RGC grant (N_HKUST620/11), the University Grants Committee of Hong Kong (AoE/P-03/08), the grant of HKUST (SRFI11SC03PG, RPC11SC09), and the National Science Foundation of China (21104044, 20974028). W. Z. Yuan thanks the support from Ph.D. Programs Foundation of Ministry of Education of China (20110073120040) and the Start-up Foundation for New Faculties of Shanghai Jiao Tong University.

Notes and references

1 (*a*) A. R. Hirst, B. Escuder, J. F. Miravet and D. K. Smith, *Angew. Chem., Int. Ed.*, 2008, **47**, 8002; (*b*) A. P. H. J. Schenning, P. Jonkheijm, E. Peeters and E. W. Meijer, *J. Am. Chem. Soc.*, 2001, **123**, 409.
2 (*a*) L. Zang, Y. K. Che and J. S. Moore, *Acc. Chem. Res.*, 2008, **41**, 1596; (*b*) J. Fang, *J. Mater. Chem.*, 2007, **17**, 3479.
3 (*a*) F. J. M. Hoeben, P. Jonkheijm, E. W. Meijer and A. P. H. J. Schenning, *Chem. Rev.*, 2005, **105**, 1491; (*b*) J. J. L. M. Cornelissen, A. E. Rowan, R. J. M. Nolte and N. A. J. M. Sommerdijk, *Chem. Rev.*, 2001, **101**, 4039; (*c*) M. Enomoto, A. Kishimura and T. Aida, *J. Am. Chem. Soc.*, 2001, **123**, 5608; (*d*) S. Kawano, N. Fujita and S. Shinkai, *J. Am. Chem. Soc.*, 2004, **126**, 8592.
4 (*a*) V. Percec, J. G. Rudick, M. Peterca and P. A. Heiney, *J. Am. Chem. Soc.*, 2008, **130**, 7503; (*b*) A. Khan, C. Kaiser and S. Hecht, *Angew. Chem., Int. Ed.*, 2006, **45**, 1878; (*c*) L. C. Palmer and S. I. Stupp, *Acc. Chem. Res.*, 2008, **41**, 1674; (*d*) J. P. Hill, W. Jin, A. Kosaka, T. Fukushima, H. Ichihara, T. Shimomura, K. Ito, T. Hashizume, N. Ishii and T. Aida, *Science*, 2004, **304**, 1481.
5 (*a*) V. Percec, M. R. Imam, M. Peterca, D. A. Wilson and P. A. Heiney, *J. Am. Chem. Soc.*, 2009, **131**, 1294; (*b*) H.-A. Klok, J. J. Hwang, S. N. Iyer and S. I. Stupp, *Macromolecules*, 2002, **35**, 746; (*c*) V. Percec, A. E. Dulcey, V. S. K. Balagurusamy, Y. Miura, J. Smidrkal, M. Peterca, S. Nummelin, U. Edlund, S. D. Hudson, P. A. Heiney, H. Duan, S. N. Magonov and S. A. Vinogradov, *Nature*, 2004, **430**, 764.
6 (*a*) H. Engelkamp, S. Middelbeek and R. J. M. Nolte, *Science*, 1999, **284**, 785; (*b*) A. Ajayaghosh and V. K. Praveen, *Acc. Chem. Res.*, 2007, **40**, 644; (*c*) C. C. Lee, C. Grenier, E. W. Meijer and A. P. H. J. Schenning, *Chem. Soc. Rev.*, 2009, **38**, 671.
7 (*a*) X. Zhang, X. Liu, R. Lu, H. Zhang and P. Gong, *J. Mater. Chem.*, 2012, **22**, 1167; (*b*) Z. Huang, S.-K. Kang and M. Lee, *J. Mater. Chem.*, 2011, **21**, 15327; (*c*) Y.-b. Lim and M. Lee, *J. Mater. Chem.*, 2008, **18**, 723; (*d*) A. Jatsch, E.-K. Schillinger, S. Schmid and P. Bäuerle, *J. Mater. Chem.*, 2010, **20**, 3563; (*e*) P. G. A. Janssen, P. Jonkheijm, P. Thordarson, J. C. Gielen, P. C. M. Christianen, J. L. J. van Dongen, E. W. Meijer and A. P. H. J. Schenning, *J. Mater. Chem.*, 2007, **17**, 2654.
8 (*a*) J. Chai and J. M. Buriak, *ACS Nano*, 2008, **2**, 489; (*b*) H. Wei, X. Zhang, C. Cheng, S.-X. Cheng and R.-X. Zhuo, *Biomaterials*, 2007, **28**, 99.
9 (*a*) A. D. Bangham and R. W. Horne, *J. Mol. Biol.*, 1964, **8**, 660; (*b*) J. Barauskas, M. Johnsson and F. Tiberg, *Nano Lett.*, 2005, **5**, 1615; (*c*) M. Antonietti and S. Föster, *Adv. Mater.*, 2003, **15**, 1323.
10 D. Lensen, D. M. Vriezema and J. C. M. van Hest, *Macromol. Biosci.*, 2008, **8**, 991.
11 (*a*) S. C. Zimmerman, F. Zeng, D. E. C. Reichert and S. V. Kolotuchin, *Science*, 1996, **271**, 1095; (*b*) S. D. Hudson, H.-T. Jung, V. Percec, W.-D. Cho, G. Johansson, G. Ungar and V. S. K. Balagurusamy, *Science*, 1997, **278**, 449.
12 (*a*) R. Iwaura, K. Yoshida, M. Masuda, K. Yase and T. Shimizu, *Chem. Mater.*, 2002, **14**, 3047; (*b*) M. Tanaka, T. Ikeda, J. Mack, N. Kobayashi and T. Haino, *J. Org. Chem.*, 2011, **76**, 5082; (*c*) S. Qu, L. Wang, X. Liu and M. Li, *Chem.–Eur. J.*, 2011, **17**, 3512.
13 (*a*) J. F. Hulvat, M. Sofos, K. Tajima and S. I. Stupp, *J. Am. Chem. Soc.*, 2005, **127**, 366; (*b*) F. Camerel, L. Bonardi, M. Schmutz and R. Ziessel, *J. Am. Chem. Soc.*, 2006, **128**, 4548.
14 K. V. Rao and S. J. George, *Org. Lett.*, 2010, **12**, 2656.
15 (*a*) F. Würthner, *Angew. Chem., Int. Ed.*, 2001, **40**, 1037; (*b*) A. P. H. J. Schenning and E. W. Meijer, *Chem. Commun.*, 2005, 3245; (*c*) A. Ajayaghosh, S. J. George and A. P. H. J. Schenning, *Top. Curr. Chem.*, 2005, **258**, 83; (*d*) T. Ishi-i and S. Shinkai, *Top.*

Curr. Chem., 2005, **258**, 119; (*e*) J. Wu, W. Pisula and K. Müllen, *Chem. Rev.*, 2007, **107**, 718; (*f*) A. Mishra, C.-Q. Ma and P. Bäuerle, *Chem. Rev.*, 2009, **109**, 1141; (*g*) Z. Chen, A. Lohr, C. R. Saha-Möller and F. Würthner, *Chem. Soc. Rev.*, 2009, **38**, 564.
16 (*a*) F. Garnier, G. Horowitz, X. Peng and D. Fichou, *Adv. Mater.*, 1990, **2**, 592; (*b*) S. Zhang, Y. Guo, Y. Zhang, R. Liu, Q. Li, X. Zhan, Y. Liu and W. Hu, *Chem. Commun.*, 2010, **46**, 2841.
17 J. H. Kim, A. Watanabe, J. W. Chung, Y. Jung, B.-K. An, H. Tada and S. Y. Park, *J. Mater. Chem.*, 2010, **20**, 1062.
18 F. Geiger, M. Stoldt, H. Schweizer, P. Bäuerle and E. Umbach, *Adv. Mater.*, 1993, **5**, 922.
19 N. Noma, T. Tsuzuki and Y. Shirota, *Adv. Mater.*, 1995, **7**, 647.
20 L. Magginia and D. Bonifazi, *Chem. Soc. Rev.*, 2012, **41**, 211.
21 S.-J. Yoon, J. H. Kim, K. S. Kim, J. W. Chung, B. Heinrich, F. Mathevet, P. Kim, B. Donnio, A.-J. Attias, D. Kim and S. Y. Park, *Adv. Funct. Mater.*, 2012, **22**, 61.
22 (*a*) E. Lee, B. Hammer, J.-K. Kim, Z. Page, T. Emrick and R. C. Hayward, *J. Am. Chem. Soc.*, 2011, **133**, 10390; (*b*) D.-J. Hong, E. Lee and M. Lee, *Chem. Commun.*, 2007, 1801; (*c*) Z. Huang, E. Lee, H.-J. Kima and M. Lee, *Chem. Commun.*, 2009, 6819.
23 (*a*) S. J. George and A. Ajayaghosh, *Chem.–Eur. J.*, 2005, **11**, 3217; (*b*) S. Ramakrishna, K. Fujihara, W.-E. Teo, T. Yong, Z. Ma and R. Ramaseshan, *Mater. Today*, 2006, **9**, 40.
24 *Nanofibers*, ed. A. Kumar, Intech, Olajnica, 2010.
25 (*a*) M. Schiek, F. Balzer, K. Al-Shamery, J. R. Brewer, A. Lützen and H.-G. Rubahn, *Small*, 2008, **4**, 176; (*b*) J. Brewer, M. Schiek, A. Lu1tzen, K. Al-Shamery and H.-G. Rubahn, *Nano Lett.*, 2006, **6**, 2656; (*c*) F. Quochi, F. Cordella, A. Mura, G. Bongiovanni, F. Balzer and H.-G. Rubahn, *Appl. Phys. Lett.*, 2006, **88**, 041106–1.
26 (*a*) K. B. An, D. S. Lee, J. S. Lee, Y. S. Park, H. S. Song and S. Y. Park, *J. Am. Chem. Soc.*, 2004, **126**, 10232; (*b*) B.-K. An, S. H. Gihm, J. W. Chung, C. R. Park, S.-K. Kwon and S. Y. Park, *J. Am. Chem. Soc.*, 2009, **131**, 3950.
27 (*a*) S. Fery-Forgues and C. Fournier-Noël, Organic Fluorescent Nanofibers and Submicrometer Rods, in *Nanofibers*, ed. A. Kumar, Intech, Olajnica, 2010; (*b*) M. Mille, J.-F. Lamère, F. Rodrigues and S. Fery-Forgues, *Langmuir*, 2008, **24**, 2671; (*c*) J. Chahine, N. Saffon, M. Cantuel and S. Fery-Forgues, *Langmuir*, 2011, **27**, 2844.
28 (*a*) B. Law, R. Weissleder and C.-H. Tung, *Bioconjugate Chem.*, 2007, **18**, 1701; (*b*) R. Malik, S. Qian and B. Law, *Anal. Biochem.*, 2011, **412**, 26.
29 F. Di Maria, P. Olivelli, M. Gazzano, A. Zanelli, M. Biasiucci, G. Gigli, D. Gentili, P. D'Angelo, M. Cavallini and G. Barbarella, *J. Am. Chem. Soc.*, 2011, **133**, 8654.
30 T. Naddo, Y. Che, W. Zhang, K. Balakrishnan, X. Yang, M. Yen, J. Zhao, J. S. Moore and L. Zang, *J. Am. Chem. Soc.*, 2007, **129**, 6978.
31 A. Wicklein, S. Ghosh, M. Sommer, F. Würthner and M. Thelakkat, *ACS Nano*, 2009, **3**, 1107.
32 J. Xiao, B. Yang, J. I. Wong, Y. Liu, F. Wei, K. J. Tan, X. Teng, Y. Wu, L. Huang, C. Kloc, F. Boey, J. Ma, H. Zhang, H. Y. Yang and Q. Zhang, *Org. Lett.*, 2011, **13**, 3004.
33 (*a*) J. B. Birks, *Photophysics of Aromatic Molecules*, Wiley, London, 1970; (*b*) E. A. Silinsh, *Organic Molecular Crystals*, Springer-Verlag, Berlin, 1980.
34 (*a*) Y. Hong, J. W. Y. Lam and B. Z. Tang, *Chem. Soc. Rev.*, 2011, **40**, 5361; (*b*) Y. Hong, J. W. Y. Lam and B. Z. Tang, *Chem. Commun.*, 2009, 4332; (*c*) J. Liu, J. W. Y. Lam and B. Z. Tang, *Chem. Rev.*, 2009, **109**, 5799; (*d*) J. Liu, J. W. Y. Lam and B. Z. Tang, *J. Inorg. Organomet. Polym. Mater.*, 2009, **19**, 249; (*e*) Z. Zhao, J. W. Y. Lam and B. Z. Tang, *Curr. Org. Chem.*, 2010, **14**, 2109; (*f*) W. Z. Yuan, S. Chen, J. W. Y. Lam, C. Deng, P. Lu, H. H.-Y. Sung, I. D. Williams, H. S. KwoK, Y. Zhang and B. Z. Tang, *Chem. Commun.*, 2011, **47**, 11216; (*g*) W. Z. Yuan, Z.-Q. Yu, Y. Tang, J. W. Y. Lam, N. Xie, P. Lu, E.-Q. Chen and B. Z. Tang, *Macromolecules*, 2011, **44**, 9618; (*h*) W. Z. Yuan, Z.-Q. Yu, P. Lu, C. Deng, J. W. Y. Lam, Z. Wang, E.-Q. Chen, Y. Ma and B. Z. Tang, *J. Mater. Chem.*, 2012, **22**, 3323; (*i*) W. Z. Yuan, X. Y. Shen, H. Zhao, J. W. Y. Lam, L. Tang, P. Lu, C. Wang, Y. Liu, Z. Wang, Q. Zheng, J. Z. Sun, Y. Ma and B. Z. Tang, *J. Phys. Chem. C*, 2010, **114**, 6090.
35 W. Z. Yuan, H. Zhao, X. Y. Shen, F. Mahtab, J. W. Y. Lam, J. Z. Sun and B. Z. Tang, *Macromolecules*, 2009, **42**, 9400.
36 R. Gujadhur, D. Venkataraman and J. T. Kintigh, *Tetrahedron Lett.*, 2001, **42**, 4791.
37 W. Humphrey, A. Dalke and K. Schulten, *J. Mol. Graphics*, 1996, **14**, 33.
38 M. Banerjee, S. J. Emond, S. V. Lindeman and R. Rathore, *J. Org. Chem.*, 2007, **72**, 8054.
39 (*a*) W. Z. Yuan, P. Lu, S. Chen, J. W. Y. Lam, Z. Wang, Y. Liu, H. S. Kwok and B. Z. Tang, *Adv. Mater.*, 2010, **22**, 2159; (*b*) Y. Liu, S. Chen, J. W. Y. Lam, P. Lu, R. T. K. Kwok, F. Mahtab, H. S. Kwok and B. Z. Tang, *Chem. Mater.*, 2011, **23**, 2536.
40 (*a*) Z. Zhao, S. Chen, X. Shen, M. Faisal, Y. Yu, P. Lu, J. W. Y. Lam, H. S. Kwok and B. Z. Tang, *Chem. Commun.*, 2010, **46**, 686; (*b*) J. Wang, J. Mei, W. Yuan, P. Lu, A. Qin, J. Sun, Y. Ma and B. Z. Tang, *J. Mater. Chem.*, 2011, **21**, 4056.
41 (*a*) J. Luo, Z. Xie, J. W. Y. Lam, L. Cheng, H. Chen, C. Qiu, H. S. Kwok, X. Zhan, Y. Liu, D. Zhu and B. Z. Tang, *Chem. Commun.*, 2001, 1740; (*b*) Y. Hong, M. Haeussler, J. W. Y. Lam, Z. Li, K. K. Sin, Y. Dong, H. Tong, J. Liu, A. Qin, R. Renneberg and B. Z. Tang, *Chem.–Eur. J.*, 2008, **14**, 6428; (*c*) H. Tong, Y. Hong, Y. Dong, Y. Ren, M. Haeussler, J. W. Y. Lam, K. S. Wong and B. Z. Tang, *J. Phys. Chem. B*, 2007, **111**, 2000; (*d*) Q. Zeng, Z. Li, Y. Dong, C. Di, A. Qin, Y. Hong, L. Ji, Z. Zhu, C. K. W. Jim, G. Yu, Q. Li, Z. Li, Y. Liu, J. Qin and B. Z. Tang, *Chem. Commun.*, 2007, 70; (*e*) Y. Liu, Y. Tang, N. N. Barashkov, I. S. Irgibaeva, J. W. Y. Lam, R. Hu, D. Birimzhanova, Y. Yu and B. Z. Tang, *J. Am. Chem. Soc.*, 2010, **132**, 13951; (*f*) Z. Li, Y. Q. Dong, J. W. Y. Lam, J. Sun, A. Qin, M. Häußler, Y. P. Dong, H. H. Y. Sung, I. D. Williams, H. S. Kwok and B. Z. Tang, *Adv. Funct. Mater.*, 2009, **19**, 905; (*g*) B. Xu, Z. Chi, Z. Yang, J. Chen, S. Deng, H. Li, X. Li, Y. Zhang, N. Xu and J. Xu, *J. Mater. Chem.*, 2010, **20**, 4135.
42 K. Jang, L. V. Brownell, P. M. Forster and D.-C. Lee, *Langmuir*, 2011, **27**, 14615.
43 Q. Dai, W. Liu, L. Zeng, C.-S. Lee, J. Wu and P. Wang, *CrystEngComm*, 2011, **13**, 4617.
44 B. Xu, J. He, Y. Dong, F. Chen, W. Yu and W. Tian, *Chem. Commun.*, 2011, **47**, 6602.
45 (*a*) Y. Dong, J. W. Y. Lam, A. Qin, Z. Li, J. Sun, Y. Dong and B. Z. Tang, *J. Inorg. Organomet. Polym. Mater.*, 2007, **17**, 673; (*b*) Y. Dong, J. W. Y. Lam, A. Qin, J. Sun, J. Liu, Z. Li, J. Sun, H. H. Y. Sung, I. D. Williams, H. S. Kwok and B. Z. Tang, *Chem. Commun.*, 2007, 3255.